Aqueous Proteomic and Metabolomic Profiles in Low-Energy vs High-Energy Femtosecond Laser-Assisted Cataract Surgery

Chang Liu,[1] Xinyue Wang,[2] Hon Shing Ong,[1,3,4] Marcus Ang,[1,3,4] Soon-Phaik Chee,[1,3–5] Jianhong Ching,[4,6] Kee Voon Chua,[4] Sharon Hong Yu Han,[4] Jodhbir S. Mehta,[1,3,4] Lei Zhou,[7,8] and Yu-Chi Liu[1,3,4,9]

[1]Singapore Eye Research Institute, Singapore
[2]School of Optometry, The Hong Kong Polytechnic University, Hong Kong
[3]Singapore National Eye Centre, Singapore
[4]Duke-NUS Medical School, Singapore
[5]Yong Loo Lin School of Medicine, National University of Singapore, Singapore
[6]KK Research Centre, KK Women's and Children's Hospital, Singapore
[7]School of Optometry; Department of Applied Biology and Chemical Technology, Research Centre for SHARP Vision (RCSV), The Hong Kong Polytechnic University, Hong Kong
[8]Centre for Eye and Vision Research (CEVR), 17W Hong Kong Science Park, Hong Kong
[9]National Taiwan University, Taiwan

Correspondence: Yu-Chi Liu, Singapore National Eye Centre, The Academia, 20 College Rd., Discovery Tower, Level 6, Singapore 169856, Singapore; liuchiy@gmail.com.
Lei Zhou, HJ503, School of Optometry, The Hong Kong Polytechnic University, Hung Hom, Kowloon 100 HKD, Hong Kong; lei.henry.zhou@polyu.edu.hk.

CL and XW contributed equally to this work and shared co-first authorship.

Received: June 24, 2024
Accepted: December 12, 2024
Published: January 7, 2025

Citation: Liu C, Wang X, Ong HS, et al. Aqueous proteomic and metabolomic profiles in low-energy vs high-energy femtosecond laser-assisted cataract surgery. *Invest Ophthalmol Vis Sci.* 2025;66(1):10. https://doi.org/10.1167/iovs.66.1.10

Purpose. To investigate the aqueous proteomics and metabolomics in low-energy and high-energy femtosecond laser-assisted cataract surgery (FLACS).

Methods. In this prospective observational study, 72 patients were randomized to 3 groups: low-energy FLACS, high-energy FLACS, and conventional phacoemulsification (controls). Aqueous was collected after femtosecond laser treatment or at the beginning of surgery (controls). Proteomic analysis was conducted using a data-independent acquisition method, whereas aqueous metabolomics were analyzed with liquid chromatography-tandem mass spectrometry. Bioinformatics analyses were performed to integrate the results of proteomics and metabolomics.

Results. Compared with low-energy FLACS, significantly elevated aqueous hemoglobin subunit beta, G protein subunit beta, carbonic anhydrase 1, and asymmetric dimethylarginine were observed in high-energy FLACS, suggesting significantly greater oxidative stress, inflammation, immunity, metabolism, and mitochondrial fatty acids oxidation. Compared with controls, significantly increased aqueous proteins and metabolites related to immune and inflammation (beta-crystallin B1, hemoglobin subunit beta, putrescine, and spermine) and oxidative stress (heat shock proteins, peroxiredoxins, and long-chain acylcarnitines) were observed in FLACS. Joint pathway analysis revealed nicotinate/nicotinamide metabolism and riboflavin metabolism were significantly overexpressed in high-energy FLACS compared with low-energy FLACS, whereas the pentose phosphate pathway and glycolysis were the most significant pathways when comparing FLACS with controls.

Conclusions. FLACS induced higher immunological and inflammatory responses, oxidative stress reactions, and mitochondrial fatty acid oxidative stress compared with controls. These differential effects were more pronounced when a higher laser energy was used.

Keywords: aqueous humor, proteomics, metabolomics, low-energy femtosecond laser-assisted cataract surgery, high-energy femtosecond laser-assisted cataract surgery

Cataract affects approximately 95 million individuals globally.[1] Femtosecond laser-assisted cataract surgery (FLACS) is a recent advancement in cataract surgery,[2] allowing for the creation of clear corneal incisions, anterior capsulotomy, and nuclear fragmentation.[1,3] Previous studies have demonstrated that FLACS is safe and effective, with comparable visual and refractive outcomes compared with conventional phacoemulsification.[4,5] Moreover, FLACS presents several potential advantages over conventional surgery, such as precise capsulotomy and decreased ultrasound energy use.[6] These benefits are particularly important in certain clinical situations, such as intumescent or dense cataracts, low corneal endothelial cell counts, and weakened zonules. Although several meta-analysis studies have reported the comparisons of the postoperative complications between conventional phacoemulsification and FLACS,[7–9] molecular

data, particularly proteomic profiles in these two surgical types, are still lacking.

Among the five current femtosecond laser (FSL) platforms approved for FLACS, the Femto LDV Z8 (Ziemer Ophthalmic Systems AG, Port, Switzerland) is the only low-energy (nJ/pulse) system that uses small size laser spots with high repetition rate (>1 MHz). Studies comparing high- and low-energy laser systems on FLACS are scarce. One clinical study reported that the Femto LDV Z8 system performed significantly better than a high-energy platform (LenSx; Alcon Laboratories, Inc., Fort Worth, TX) in terms of completeness of capsulotomy (100% vs 94%) and intraoperative miosis (0% vs 19%).[10] However, the underlying molecular mechanisms accounting for these clinical observations are poorly understood.

Previous studies have shown that compared with conventional phacoemulsification, FLACS induced significantly higher aqueous prostaglandin E_2, interleukin (IL) 1 receptor antagonist, IL-6, IL-8, interferon-γ, and free radicals,[11–15] which are associated with intraoperative miosis and postoperative inflammatory response. These findings underscore the clinical implications of understanding the aqueous molecular profiles more comprehensively. Advanced quantitative proteomics and metabolomics are emerging as potentially powerful tools in ophthalmology research,[16,17] offering high reproducibility and accuracy in elucidating the functions and interactions of proteins and metabolites within biological systems.[18] Integrative analysis of both proteins and metabolites will contribute to an in-depth interpretation of underlying biological phenomena.[19] Aqueous humor has been used in proteomic and metabolomic analyses to identify biomarkers for several eye diseases, such as uveitis, dry eye, and keratoconus.[18,20]

To our knowledge, there are no studies published on the aqueous metabolomic and proteomic profiles, or their associated biological responses, in patients undergoing FLACS, particularly in the comparison between low- and high-energy FSL platforms. Deciphering these differences could provide better insight into the impact of FLACS on the tissue at a molecular level and potential clinical implications.

Methods

Study Populations

This prospective study recruited 72 eyes of 72 patients with age-related cataracts who met the indications of cataract surgery at Singapore National Eye Centre from January 2023 to June 2023. The exclusion criteria were diabetes, autoimmune diseases, the use of nonsteroidal anti-inflammatory drugs within 3 months from the time of surgery, a history of ocular surgery or trauma, and active ocular copathologies that might affect the aqueous analysis, such as uveitis and cystoid macular edema (CME). Patients were randomized to three groups: (1) FLACS with the Catalys system (Johnson & Johnson, NJ; high-energy group); (2) FLACS with the LDV Z8 system (low-energy group); and (3) conventional phacoemulsification, serving as controls. The cataract severity was graded with the Lens Opacity Classification System III.[21] Approval for the study was granted by the Institutional Review Board of SingHealth, Singapore (Number:2021/2699). The study was conducted in accordance with the Declaration of Helsinki and informed consent was obtained from all participants.

Surgical Technique and Aqueous Humor Collection

All procedures were performed under local anesthesia with sedation. The FLACS with the LDV Z8 system was conducted as previously described.[12,22] Briefly, the suction ring was applied, and a fluid–patient interface was used.[23] Laser pretreatment at 1 MHz with pulse energy in the nano-Joule range started with an anterior capsulotomy with a preset diameter of 5.0 mm, followed by lens fragmentation with a six-sector pie-cut pattern, and then a 2.6-mm corneal incision. For the FLACS with the Catalys system, the docking process was similar, with a suction ring followed by the application of liquid before the laser head docking.[24] FSL at KHz with pulse energy in micro-Joule range operated a size of 5.0 mm anterior capsulotomy, lens fragmentation, and then a 2.6-mm manual corneal incision. In FLACS eyes, approximately 100 to 150 µL of aqueous was collected using a 30G needle within 5 minutes of the completion of laser pretreatment. For controls, the aqueous was collected identically before creating the corneal incision. All aqueous samples were immediately placed on ice for transportation to the laboratory, which were subsequently stored at –80°C until analysis. The phacoemulsification was performed subsequently using the same machine (Centurion Vision system, Alcon Laboratories, Inc.), and an IOL (SA60AT, Alcon; or ZCB00, Johnson & Johnson Vision) was implanted. Preoperative and postoperative regimens were prescribed as previously described and were identical in all patients.[12]

Clinical Assessments

At 1 day postoperatively, anterior chamber inflammation was graded from 0 to 4 following the Standardization of Uveitis Nomenclature Working Group grading scheme.[25]

Aqueous Proteomic Profiles Analysis

Lysis buffer (EasyPep Mini MS Sample Prep Kit, Thermo Fisher Scientific, Waltham, MA) was used to extract the proteins.[26] The lysates were centrifuged, and protein quantitation was performed using DC Protein Assay (Bio-Rad Laboratories Inc., Hercules, CA) and normalized with the total protein amount. The protein solutions were then reduced, alkylated, digested, and cleaned-up according to the manufacturer's instruction (EasyPep Mini MS Sample Prep Kit, Thermo Fisher Scientific). Peptides were reconstituted in 2% acetonitrile, 0.1% formic acid in water and peptide concentration was determined by Thermo Fisher Scientific Pierce Quantitative Fluorescent Peptide Assay.[27] iRT standard (Biognosys AG, Schlieren, Switzerland) was spiked to reconstituted peptide sample. The peptide samples were then analyzed on an EASY-nLiquid chromatography 1200 system coupled to Orbitrap Exploris 480 mass spectrometer (Thermo Fisher Scientific). An equal amount of total peptide (1 µg) from each sample was injected for the proteomics analysis. The Easy-nLiquid chromatography system was equipped with an in-line trap column of PepMap 100 C18, 3 µm, 75 µm × 2 cm, and Easy-spray Pepmap RSLC C18, 2 µm, 25 cm × 75 µm column. The EASY-nLiquid chromatography was operated at a flow rate of 300 nL/min. Mobile phase A consisted of 0.1% formic acid in water and mobile phase B was made up of 0.1%formic acid, 80% acetonitrile in water. A step gradient was used from 5% to

Investigative Ophthalmology & Visual Science

18% mobile phase B for 35 minutes, followed by 20 minutes from 18% to 50%, and last 5 minutes from 50% to 95% solvent B. Orbitrap Exploris 480 mass spectrometer was operated in data-independent and positive ionization mode.

Aqueous Metabolomic Profiles Analysis

Aqueous metabolomic profile analysis was performed using liquid chromatography-tandem mass spectrometry. A list of the measured metabolites is presented in Supplementary Table S1. For the extraction of acylcarnitines, thawed aqueous samples (50 µL) were spiked with 15 µL deuterium-labelled acylcarnitines as internal standard, then extracted, derivatized, and ran on an Agilent 6430 Triple Quadrupole liquid chromatography/mass spectrometry system (Agilent Technologies, Santa Clara, CA) as previously described.[28] For the analysis of nitrogen-containing compounds, 23 µL of sample was spiked with a mixture of deuterium-/carbon 13-labeled amino acids, derivatized using phenyl isothiocyanate, reconstituted, then run on a Waters Xevo TQ-XS mass spectrometer (Waters Corp, Milford, MA) as described.[29] Internal standards were used to normalize metabolite levels (Supplemental Table S2).

Statistical and Bioinformatics Analysis

The differences in anterior chamber flare grading were analyzed using a Kruskal–Wallis test. Our data on the pilot 6 patients identified approximately 1700 proteins and 900 metabolites in aqueous samples. The desired fold change (FC) is >1.5 with a standard deviation of 0.60, and the acceptable false discovery rate (FDR) is 1%. The required sample size was therefore 26 eyes with a power of 80% and a 5% significance level.

For the proteomics data analysis, the resulting tandem mass spectrometry data were processed using Spectronaut 15 (Biognosys AG) with the DirectDIA algorithm. The protein expression profile was log2-transformed and normalized. For downstream data analysis, median normalization was used. Proteins with missing values in >30% of samples were excluded. Missing values in the expression profiles were imputed using the DreamAI package in R.[30] The R package sva (v 3.46.0) was employed to remove batch effects. The R package ropls (v1.30.0) was used to perform partial least squares-discriminant analysis (PLS-DA) that discriminates between FLACS and controls. PLS-DA is a robust method for visualizing and differentiating distinct groups based on their proteomic and metabolomic profiles.[31]

Differential expression analysis was conducted using the limma package (v3.54.2). Proteins with a FDR of <0.05 and a FC of >1.5 were considered differentially expressed. Metascape platform (https://metascape.org/) was used to perform Gene Set Enrichment Analysis (GSEA), including Gene Ontology, biological processes, Kyoto Encyclopedia of Genes and Genomes pathways, the Small Molecule Pathway Database, and Reactome gene sets.[32] GSEA allows the identification of biological pathways associated with a specific set of proteins and metabolites,[33] and protein network analysis explores the interactions between proteins to uncover critical networks and modules driving cellular activities.[34] The Wilcoxon signed-rank test was performed to assess the statistical significance of protein expression difference between the two groups.

The metabolomics data analysis workflow was the same as the proteomic analysis stated elsewhere in this article. Metabolites with a FDR of <0.05 and a FC of >1.2 were considered differentially expressed. MetaboAnalyst platform was used to perform Metabolite Set Enrichment Analysis, including over-representation analysis, pathway analysis (integrating pathway enrichment analysis and pathway topology analysis), and joint pathway analysis (simultaneously analyze genes and metabolites of interest).[35] We applied Data Integration Analysis for Biomarker Discovery using Latent cOmponents (DIABLO) algorithm from R package 'mixOmics' to integrate the protomics and metabolomics data based on generalized, supervised partial least-squares approach.[36,37]

Results

Patient Characteristics

Thirty-six eyes underwent low-energy FLACS, 26 eyes underwent high-energy FLACS, and 10 eyes underwent conventional phacoemulsification. Among these 3 groups, 20 (56%), 12 (46%), and 6 (60%) patients were female, respectively ($P = 0.69$). The mean ages of patients were 67.0 ± 11.0 years, 67.5 ± 9.2 years, and 66.8 ± 9.3 years, respectively ($P = 0.87$). The Opacity Classification System III grades were comparable between the three groups, with the mean grading of 2.7 ± 0.9, 2.5 ± 1.0, and 2.6 ± 0.8, respectively ($P = 0.91$). For the low-energy, high-energy, and control groups, the preoperative best-corrected distance visual acuity was comparable at 0.50 ± 0.15 logMAR, 0.45 ± 0.15 logMAR, and 0.50 ± 0.10 logMAR, respectively ($P = 0.74$). The IOP values were 18.7 ± 7.1, 17.9 ± 6.7, and 19.1 ± 7.4, respectively ($P = 0.89$). All cases underwent an uneventful surgery without intraoperative or postoperative complications.

Aqueous Proteomic Profiles Analysis

PLS-DA analysis displayed a clear separation of the aqueous proteomes of the FLACS group vs controls ($R^2Y = 0.993$) (Fig. 1A). There was also good separation between high-energy FLACS, low-energy FLACS, and controls ($R^2Y = 0.615$) (Fig. 1B).

A total of 235 significantly differential expressed proteins were identified in two FLACS groups, compared with controls (Fig. 2A, Supplementary Fig. S1A). In the FLACS group, the expression of alpha-crystallin A chain, alpha-crystallin B chain, and heat shock protein beta-1 were significantly increased (FC = 3.01, $P < 0.01$; FC = 2.71, $P < 0.01$; and FC = 1.92, $P < 0.01$, respectively). These proteins are members of the small heat shock protein family. Aqueous peroxiredoxins (PRDXs), including PRDX2 and PRDX6, were significantly increased (FC = 1.65, $P < 0.001$ and FC = 1.56, $P < 0.001$, respectively). Several proteins associated with immune and inflammatory responses, such as beta-crystallin B1 (CRBB1; FC = 2.87, $P < 0.001$), hemoglobin subunit beta (HBB; FC = 3.43, $P < 0.001$), and hemoglobin subunit delta (HBD; FC = 2.97, $P = 0.001$), were also significantly upregulated in FLACS compared with controls (Fig. 2B).

When comparing high- and low-energy FLACS, eight significantly dysregulated proteins were identified (Fig. 2C, Supplementary Fig. S1B). HBB and G protein subunit beta (GBB1), associated with immune cells, were signif-

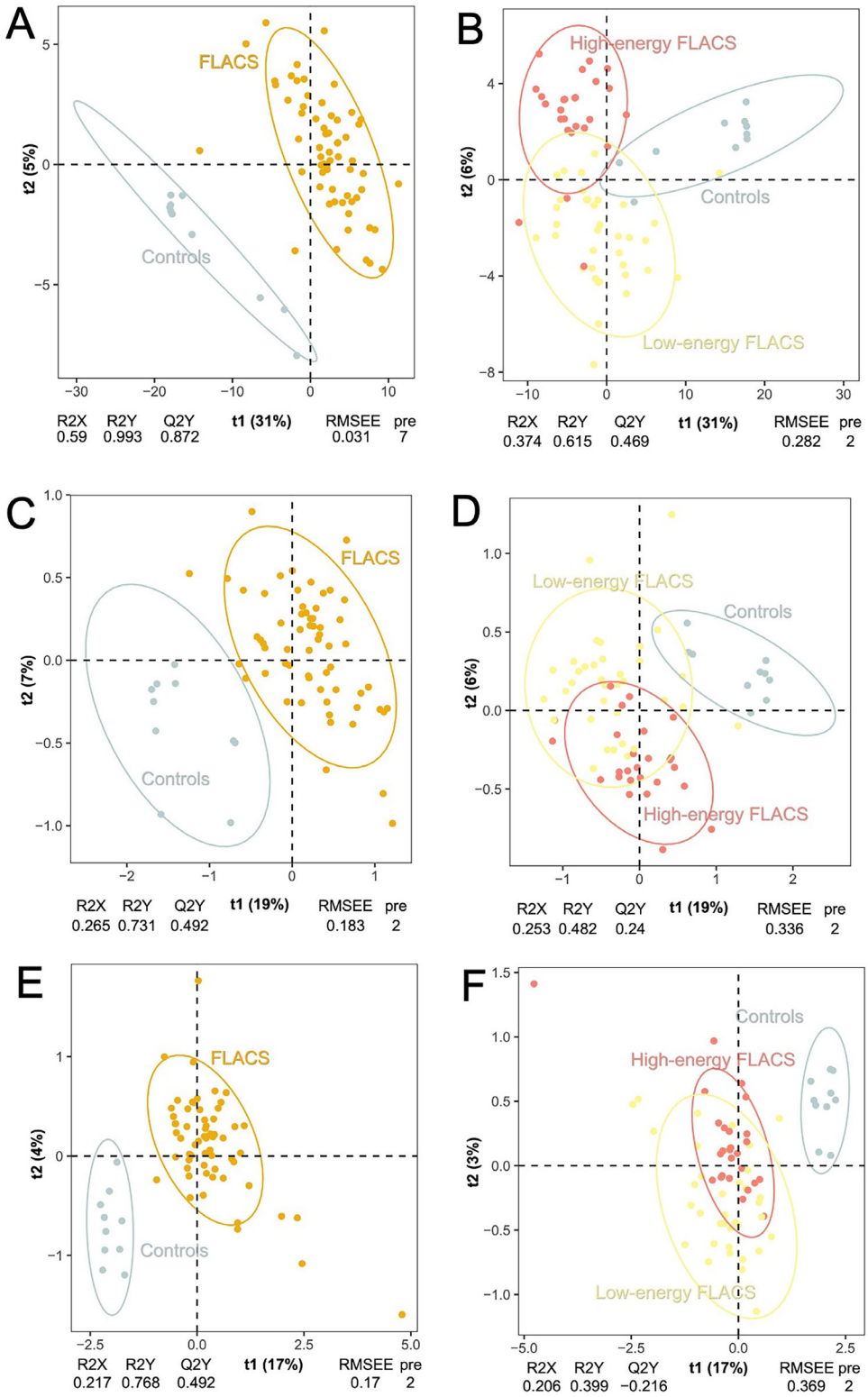

Figure 1. PLS-DA analysis of proteomics and metabolomics. Clear separation of aqueous proteomic profiles between FLACS and controls (**A**). Separation of aqueous proteomic profiles among high-energy FLACS, low-energy FLACS and controls (**B**). Distinct separation of aqueous amino acid profiles of FLACS vs controls (**C**). Separation of aqueous amino acid profiles among high-energy FLACS, low-energy FLACS, and controls (**D**). Differentiation of aqueous acylcarnitine profiles between FLACS and controls (**E**). Overlapping area of aqueous acylcarnitine profiles between high-energy FLACS and low-energy FLACS (**F**). Permutation tests showing PLS-DA models (**A**, **B**, **C**, **D**, **E**) not overfitted with goodness of prediction, while model (**F**) showing overfitted and nonpredictive.

Investigative Ophthalmology & Visual Science

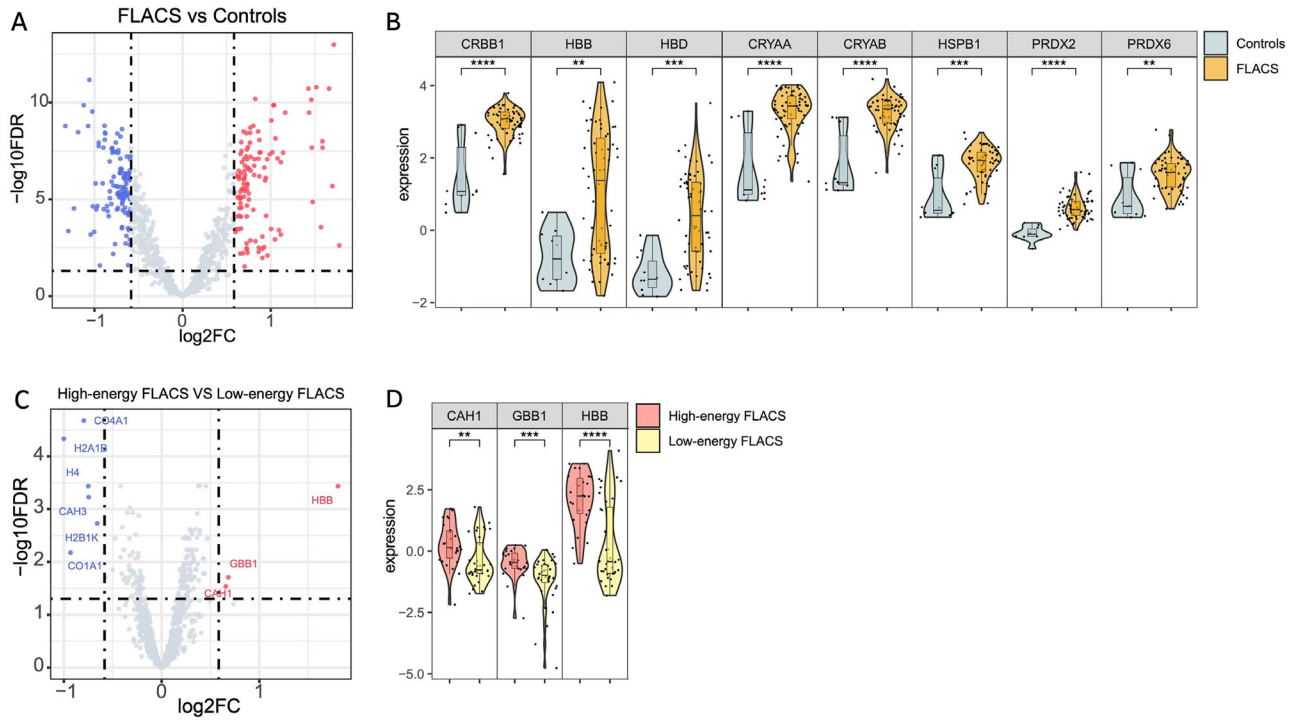

Figure 2. Aqueous proteomic profiles of FLACS vs controls, and high-energy FLACS vs low-energy FLACS. Volcano plot (**A**) presenting the −log10FDR, *y*-axis) as a function of $\log_2$FC (*x*-axis) in aqueous proteins comparing FLACS vs controls. Violin plots (**B**) displaying the representative aqueous proteins of FLACS vs controls. Volcano plot (**C**) displaying the FDR (−log10FDR, *y*-axis) as a function of $\log_2$FC (*x*-axis) in aqueous proteins between high-energy and low-energy FLACS. Violin plots (**D**) displaying the representative aqueous proteins of FLACS vs controls high-energy FLACS vs low-energy FLACS. *Red dots* represent upregulated proteins with $\log_2\text{FC} \geq 0.585$, and *blue dots* represent down-regulated proteins with $\log_2\text{FC} \leq -0.585$ in volcano plots. The significance for comparisons between different groups was examined by Wilcoxon test and labeled with * $P < 0.050$, ** $P < 0.010$, *** $P < 0.0005$, **** $P < 0.00005$ in violin plots.

Table 1. Significantly Expressed Pathways by GSEA

Terms Name	Log P	Log (q-Value)
Top 5 significantly pathways enriched by dysregulated proteins in FLACS vs controls		
Cellular responses to stress	−11.536	−8.445
M phase	−7.582	−5.400
TCF dependent signaling in response to WNT	−7.510	−5.356
Signaling by WNT	−7.348	−5.217
Signaling by NOTCH	−6.539	−4.480
Top 5 significantly pathways enriched by dysregulated proteins in high-energy FLACS vs low-energy FLACS		
Signaling by WNT	−5.773	−2.858
TCF dependent signaling in response to WNT	−4.444	−1.949
Signaling by NOTCH	−4.428	−1.938
Transcriptional regulation by RUNX1	−4.417	−1.933
Cellular responses to stress	−4.288	−1.811

icantly increased in high-energy FLACS group (FC = 3.48, $P < 0.001$ and FC = 1.60, $P = 0.002$, respectively). Significantly elevated aqueous carbonic anhydrase 1 (CAH1), implicated in metabolism and stress responses, was found in high-energy FLACS (FC = 1.58, $P = 0.004$) (Fig. 2D).

GSEA revealed that these significantly dysregulated proteins in FLACS vs controls, as well as in high-energy vs low-energy FLACS, were involved in the pathways, including T-cell factor (TCF) dependent signaling in response to Wingless-related integration site (WNT), WNT signaling, and neurogenic locus notch protein (NOTCH) signaling pathways (Table 1; Supplementary Fig. S2). Protein–protein interaction network analysis determined the key biological processes linked with the differential expressed proteins in FLACS vs controls, as well as in high-energy vs low-energy FLACS, were mainly involved in pathways, such as glycoltic process Cdk1 complex, metabolism and regulation of collagen, and metabolic process (Table 2; Fig. 3). These pathways and modules are mainly related to inflammation, immunological responses, and metabolic processes.

Table 2. Modules Identified by Protein–Protein Interaction Network Analysis

Modules in High-Energy FLACS vs Low-Energy FLACS
Glycolytic process Cdk1 complex
Metabolism and regulation of collagen
Metabolic processes
Modules in FLACS vs controls
Glycolytic process Cdk1 complex
Metabolic processes
Proteasome complex
Regulation of cellular processes and signaling
Maintaining cellular and extracellular homeostasis
Metabolism and regulation of collagen
Response to oxidative stress and the detoxification of ROS
Regulation of the complement cascade

ROS, reactive oxygen species.

Aqueous Metabolomic Profiles Analysis

PLS-DA analysis revealed distinct separations in aqueous amino acids between FLACS and controls, as well as between high and low-energy FLACS ($R^2Y = 0.731$, $R^2Y = 0.482$) (Fig. 1C, D). Similarly, PLS-DA analysis also demonstrated a clear separation in aqueous acylcarnitines between FLACS and controls (Fig. 1E).

There were 9 significantly dysregulated amino acids and 19 significantly dysregulated acylcarnitines between FLACS and controls (Fig. 4A, Supplementary Fig. S3). Laser pretreatment in FLACS led to elevated aqueous putrescine (FC = 1.22, $P < 0.001$) and spermine (FC = 1.29, $P < 0.001$), which are involved in inflammatory responses. Glutathione (FC = 1.80, $P < 0.001$), γ-aminobutyric acid (FC = 1.23, $P = 0.021$), aspartic acid (FC = 1.21, $P < 0.001$), glutamic acid (FC = 1.21, $P < 0.001$), and inosine (FC = 1.37, $P < 0.001$), which are related to ischemic stress and oxidative stress reactions, were significantly increased (Fig. 4B).

Concerning the acylcarnitine profiles, the medium and long-chain acylcarnitines, including C7-DC (heptanedioyl carnitine; FC = 1.40, $P < 0.001$), C8:1-OH/C6:1-DC (FC = 1.22, $P = 0.003$), C10 (decanoylcarnitine; FC = 1.25, $P < 0.001$), C14:1 (cis-5-tetradecenoylcarnitine; FC = 1.33, $P < 0.001$), C18:1 (elaidic carnitine; FC = 1.51, $P < 0.001$), C20:2 (FC = 1.27, $P = 0.002$), C20:4 (FC = 1.41, $P < 0.001$), C26 (FC = 1.51, $P < 0.001$), and C28 (FC = 1.31, $P < 0.001$),

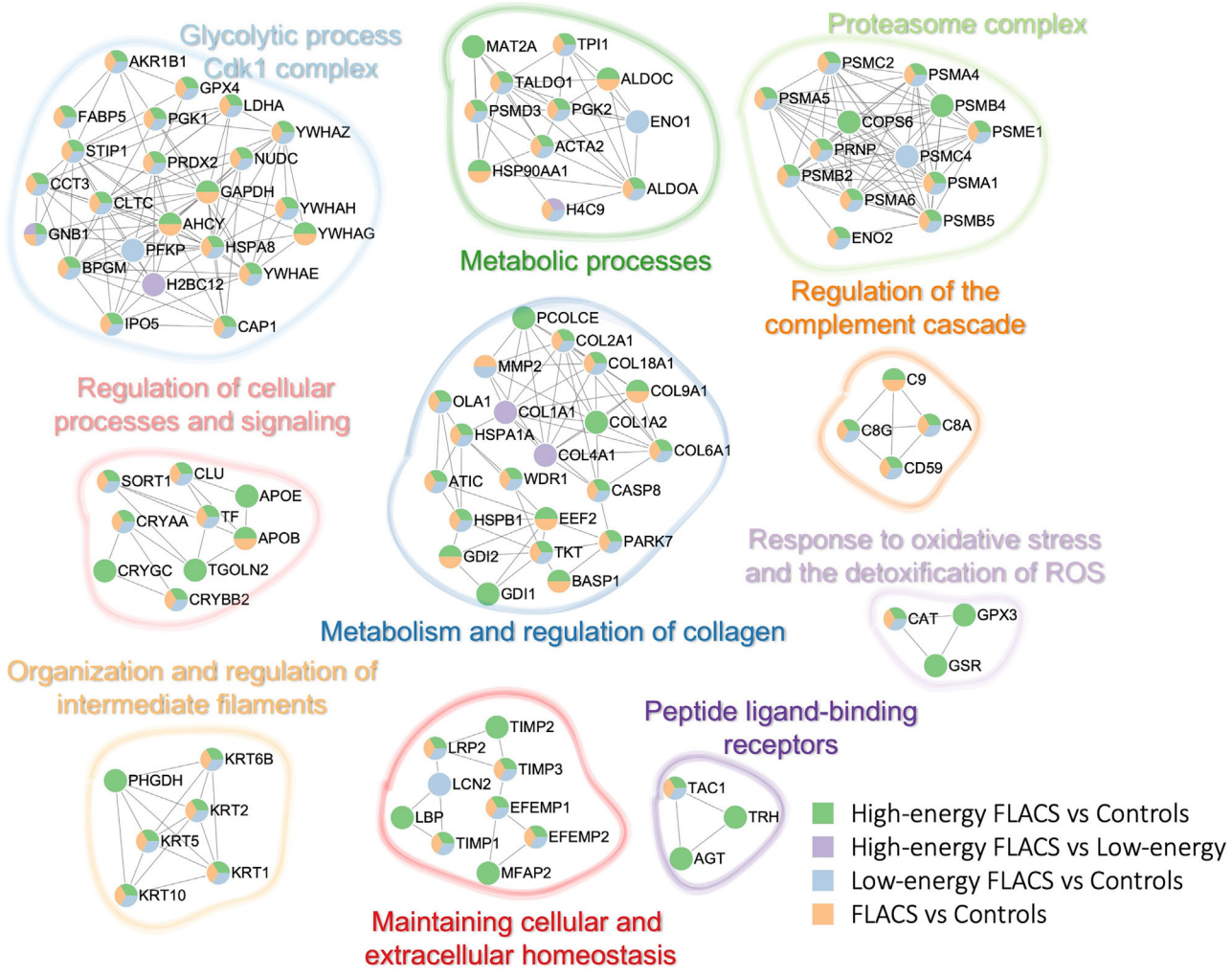

Figure 3. Protein–protein interaction network analysis of differentially expressed proteins between different groups (*yellow*, FLACS vs controls; *purple*, high vs low-energy FLACS; green, high-energy FLACS vs controls; *blue*, low-energy FLACS vs controls). ROS, reactive oxygen species.

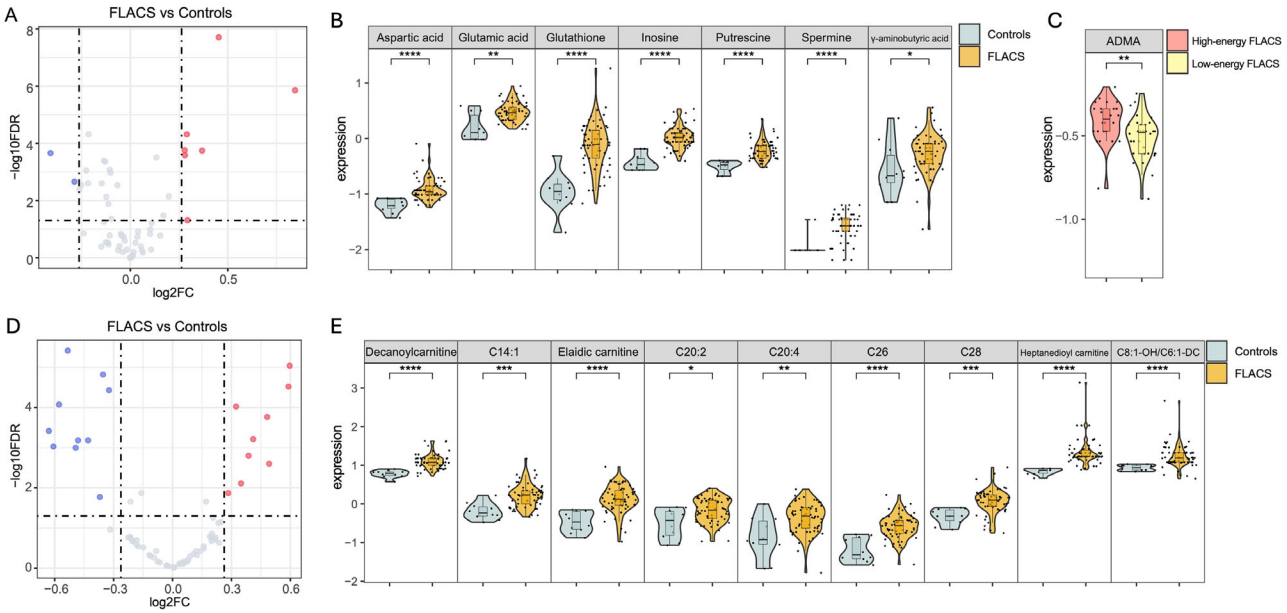

Figure 4. Aqueous metabolomics profiles of FLACS vs controls, as well as in high-energy vs low-energy FLACS. Volcano plot (**A**) presenting the FDR (−log10FDR, *y*-axis) as a function of $\log_2$FC (*x*-axis) in aqueous amino acids comparing FLACS vs controls. Violin plots showing the representative aqueous amino acids of FLACS vs controls (**B**), and high-energy vs low-energy FLACS (**C**).Volcano plot (**D**) displaying the FDR (−log10FDR, *y*-axis) as a function of $\log_2$FC (*x*-axis) in aqueous acylcarnitines, comparing FLACS vs controls. Violin plots (**E**) displaying the representative aqueous acylcarnitines in FLACS vs controls. Differential expressed metabolites with $\log_2\text{FC} \geq 0.263$ and $\log_2\text{FC} \leq -0.263$ are shown in *red dots* and *blue dots*, respectively, in volcano plots. The significance for comparisons between different groups was examined by Wilcoxon test and labeled with * $P < 0.050$, ** $P < 0.010$, *** $P < 0.0005$, ****$P < 0.00005$ in violin plots.

which are linked to mitochondrial fatty acid oxidation pathways, were significantly increased in FLACS compared with controls (Fig. 4E). When comparing high-energy FLACS and low-energy FLACS, an elevated concentration of asymmetric dimethylarginine (ADMA), which is an endogenous nitric oxide synthase inhibitor, was observed in the high-energy FLACS group (FC = 1.22, $P < 0.001$; Fig. 4C).

On the Kyoto Encyclopedia of Genes and Genomes and Small Molecule Pathway Database pathway analysis for the identified amino acids and acylcarnitines, the most significantly enriched biological processes in FLACS vs controls were d-glutamine and d-glutamate metabolism and aspartate metabolism, which were related to mitochondrial fatty acid oxidation (Fig. 5).

Integrated Analysis of Proteomics and Metabolomics

We performed DIABLO analysis on the proteomics and metabolomics data, revealing strong positive correlations between proteins and amino acids (r = 0.76), proteins and lipids (r = 0.65), as well as amino acids and lipids (r = 0.78), respectively (Fig. 6). This robust agreement underscores the significance of their consistency and suggests that the omics layers provide complementary insights into the biological processes being studied. By incorporating the proteomic and metabolomic data, we identified the common pathways associated with those significantly dysregulated proteins and metabolites. The pentose phosphate pathway (PPP) and glycolysis were the most significant joint pathways when comparing FLACS vs controls, whereas nicotinate and nicotinamide metabolism and riboflavin metabolism were the most significant joint pathways when comparing high-energy FLACS vs low-energy FLACS (Fig. 7). These pathways are associated with energy metabolism and mitochondrial oxidative stress.

Clinical Outcomes

The best-corrected distance visual acuity was comparable across the three groups postoperatively: 0.15 ± 0.05 logMAR for low energy, 0.15 ± 0.05 logMAR for high energy, and 0.15 ± 0.01 logMAR for controls ($P = 0.92$). IOP also showed comparability, measuring 19.5 ± 6.2, 19.6 ± 7.2, and 18.9 ± 6.7 for low energy, high energy, and controls, respectively ($P = 0.94$).For the postoperative anterior chamber inflammation evaluation, the majority of eye had a grade of ≤1. Four eyes (11.1%) in the low-energy group, two eyes (7.7%) in the high-energy group, and one eye (10.0%) in controls had grade >1 ($P = 0.51$).

Discussion

In the present study, we demonstrated that the FSL stage during FLACS induced aqueous immunological and inflammatory responses, oxidative stress, and mitochondrial fatty acid oxidation. More important, these reactions are more pronounced in a high-energy laser platform, compared with a low-energy platform, suggesting that laser pulse energy influences the degree of tissue inflammation, aqueous oxidative stress, and metabolic responses in FLACS. To our knowledge, this study is the first to investigate aqueous proteomics and metabolomics for FLACS, as well as for further comparisons between different FSL platforms in terms of laser energy used. We also integrated proteomic and metabolomic profiles and reported the shared common pathways, which

Investigative Ophthalmology & Visual Science

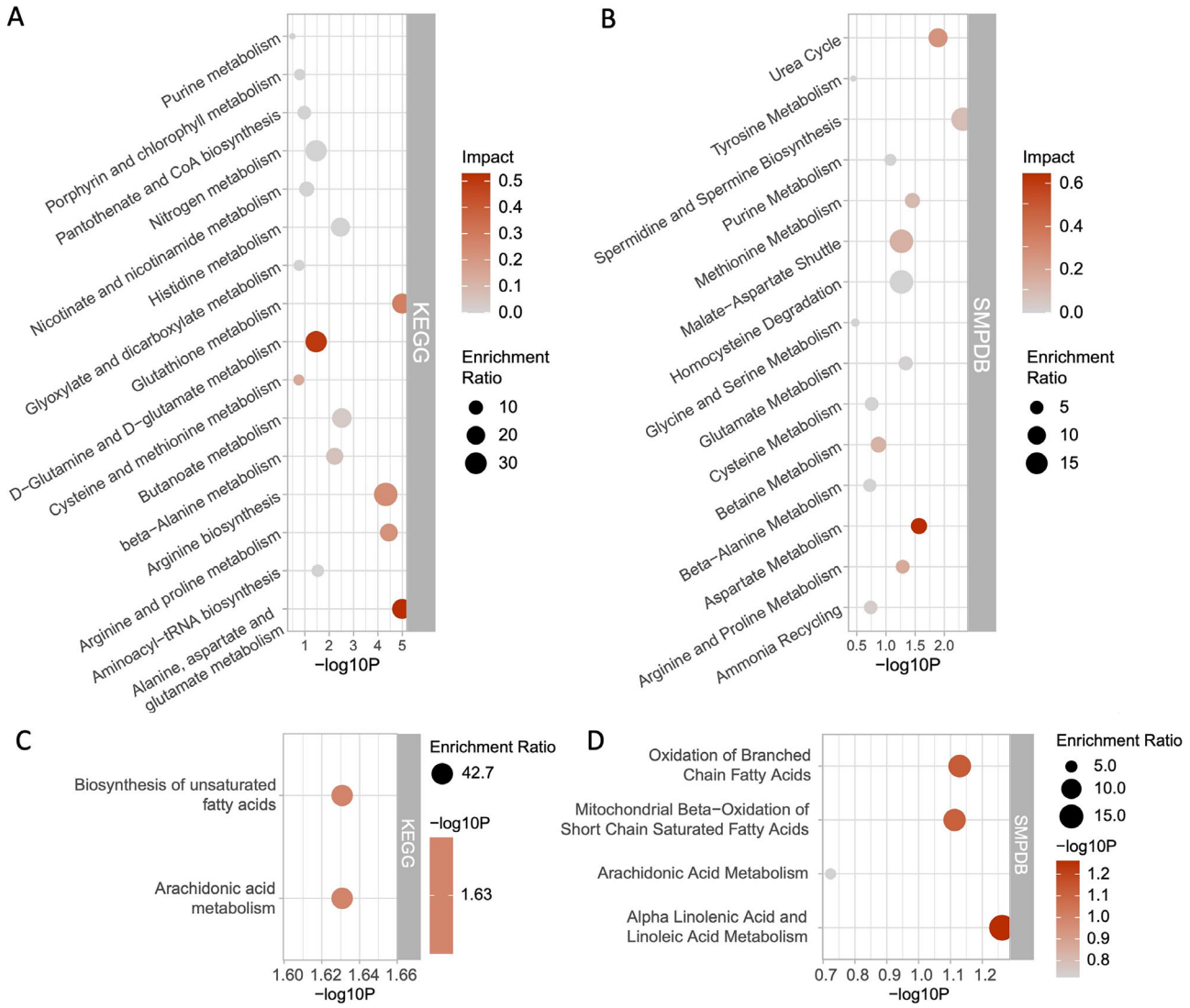

Figure 5. Metabolite set enrichment analysis. Kyoto Encyclopedia of Genes and Genomes (KEGG) and Small Molecule Pathway Database (SMPDB) pathway analysis of dysregulated amino acids (**A**, **B**) and acylcarnitines (**C**, **D**) in FLACS vs controls. The darker the color of the circle, the greater the significance.

offered a better understanding of the interplay between various biomolecules and provided deeper insight into the molecular changes induced by FSL in FLACS.

Our study showed that high-energy FSL treatment led to significantly elevated levels of HBB, GBB1, and CAH1, compared with low-energy FSL. HBB and GBB1 regulate immune cell activity and engage in cell chemotaxis.[38,39] CAH1 inhibitor could enhance antioxidant enzyme activity in aqueous.[40] These proteins are linked to overexpressed WNT, Wnt-TCF, NOTCH signaling, cellular responses to stress, and RUNX1 pathways, mediating immune cell maintenance, inflammatory response modulation, and tissue homeostasis and repair.[41–44] The protein–protein interaction network analysis also indicated that high-energy FLACS induced greater extent of immunological, inflammatory, and oxidative stress than low-energy FLACS. A low-energy laser platform uses precise placement of smaller overlapping spots with low pulse energy and a high frequency, potentially reducing damage to the surrounding tissue and resultant inflammatory responses.[45,46] Schwarzenbacher et al.[45] demonstrated that low-energy pulse lasers induced only minimal IL release compared with conventional surgery. Another two clinical studies presented that there was no occurrence of intraoperative miosis in low-energy FLACS even without the use of preoperative nonsteroidal anti-inflammatory drug.[10,47] The occurrence of postoperative CME in low-energy FLACS was lower than that in conventional phacoemulsification,[48] whereas the risk of CME development is comparable between conventional phacoemulsification and high-energy FLACS.[49] These results are consistent with our molecular findings that laser pulse energy significantly impacts the level of aqueous inflammation and oxidative stress.

In the metabolomics analysis, elevated aqueous ADMA was observed in high-energy FSL treatment compared with the low-energy one. ADMA is generated under oxidative stress conditions, and its increase has been reported in uveitis and diabetic retinopathy.[50,51] On the

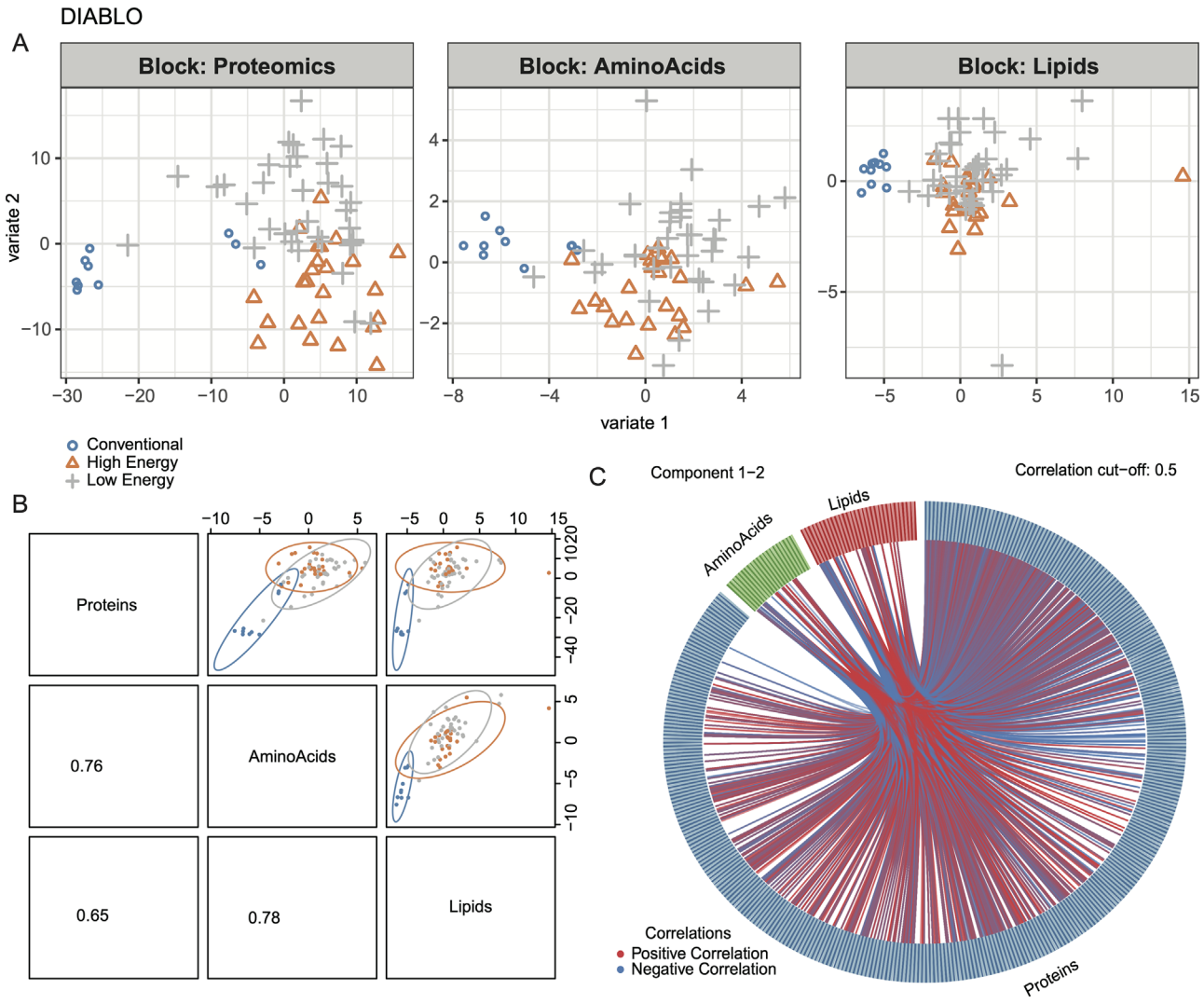

Figure 6. DIABLO analysis of proteomics and metabolomics. The plot showing the individual samples of three omics data from the DIABLO analysis, with different colors representing distinct sample groups. *Blue circle*, controls; *orange triangle*, high-energy FLACS; *gray cross*, low-energy FLACS (**A**). The correlations across three omics data based on the first component of DIABLO, displaying strong positive correlations between proteins and amino acids (r = 0.76), proteins and lipids (r = 0.65), as well as amino acids and lipids (r = 0.78) (**B**). Circos plot between proteins and metabolites with strong correlations (absolute R value > 0.5) (**C**).

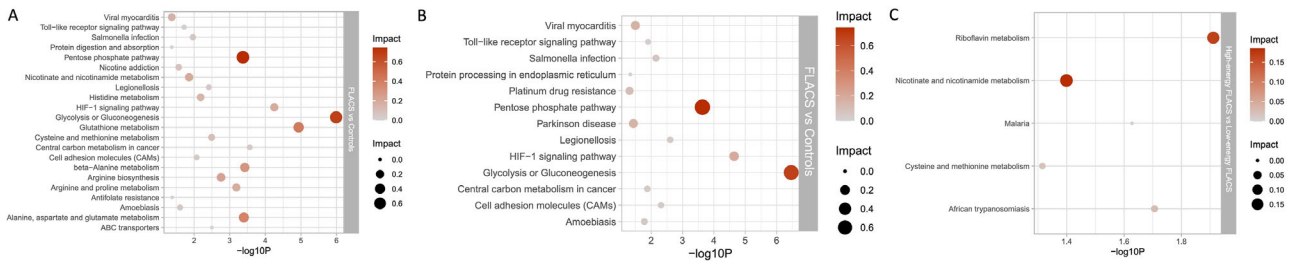

Figure 7. Joint pathway analysis of proteomics and metabolomics. Joint pathway analysis of dysregulated proteins and amino acids (**A**), dysregulated proteins and acylcarnitines (**B**) when comparing FLACS vs controls. Joint pathway analysis of dysregulated proteins and amino acids when comparing high- vs low-energy FLACS (**C**). The darker the color of the circle, the greater the significance.

joint pathway analysis of proteomic and metabolomic profiles, the higher energy of FSL was linked to riboflavin metabolism and nicotinate and nicotinamide metabolism. Both participate in the immune system, oxidation of mitochondria, and energy generation.[52,53] Taken together, these results suggested higher laser energy in FLACS intensified disruption of cell homeostasis and induced more metabolic changes and oxidative stress

responses, as well as immunological and inflammatory responses.

Compared with controls, FLACS presented with increased aqueous HBB, HBD, and CRBB1. Upregulated HBD and CRBB1 were observed in several immune and inflammatory diseases,[54] including uveitis.[55] The oxidative stress-related proteins, including heat shock proteins and PRDXs, were also significantly upregulated in the FLACS group. PRDXs, such as PRDX2 and PRDX6, protect cells from attack via reactive oxygen species and play a beneficial effect in inflammatory diseases.[56,57] These significantly expressed proteins are linked to cellular responses to stress, M phase, Wnt-TCF, and NOTCH signaling pathways, suggesting a greater extent of inflammatory and immunological reactions, active cell cycle response, metabolic processes, and oxidative stress, in FLACS than controls.

Several dysregulated amino acids were also observed in FLACS group compared with controls. Putrescine and spermine were found to be increased in acute uveitis.[58] Antioxidant glutathione, glutamic acid, aspartic acid, γ-aminobutyric acid, and inosine are recognized to exert protective effects in ocular hypoxia or ischemia.[59–62] In addition to laser-induced tissue stress, the increase in these molecules might also be due to the tissue ischemia that occurred in acute IOP elevation during the suction phase in FLACS. The elevation of these amino acids in FLACS suggested a potentially enhanced oxidative stress and tissue inflammation triggered by FSL treatment. These results were consistent with our previous randomized controlled trial, in which we reported that the FLACS group had higher aqueous prostaglandin E_2 and free radicals compared with conventional phacoemulsification.[11] On the pathway analysis, d-glutamate metabolism and aspartate metabolism, which are known to protect the body from oxidative stress and ischemia and reperfusion injury,[63] were significantly overexpressed in FLACS.

There are also nine medium- and long-chain acylcarnitines that were increased in FLACS compared with controls, and the pathways enriched by these acylcarnitines are mainly related to mitochondrial fatty acid oxidation, suggesting a subsequent dysfunction in mitochondrial metabolism and impairment of fatty acid beta-oxidation induced by FSL.[28,64,65] The finding aligns with the results of previous in vitro experiments, which have shown FSL resulted in fragmentation or swelling of mitochondria.[66] Recent studies have highlighted the changes of aqueous carnitines in various ocular diseases including diabetic retinopathy and uveitis,[20,51,67,68] suggesting a disturbance in the carnitine shuttle system and fatty acid metabolism potentially contribute to disease pathogenesis.[67,69] On the joint pathway analysis, PPP and glycolysis and gluconeogenesis were overexpressed in FLACS vs controls. PPP was activated by mitochondrial oxidative stress to maintain mitochondrial NADPH pools.[70] Glycolysis and gluconeogenesis is related to energy metabolism and regulates cellular metabolism.[71] Hence, FSL treatment resulted in stronger oxidative stress and metabolic responses.

Our findings may provide clinical implications for cataract surgery patients with underlying conditions of disrupting the blood–aqueous barrier, such as diabetes and a history of uveitis or CME, which could potentially exacerbate postoperative inflammation. Conventional phacoemulsification or low-energy FLACS can be considered in these scenarios, because they induce a lower inflammatory response from the molecular perspective.

There are several limitations to our study. The assessment of anterior chamber inflammation was performed with subjective grading rather than quantitative measurement using the laser flare cell meter, and the grading may be too crude to reflect subtle molecular changes. This factor can also explain why no significant difference in the aqueous inflammation level was observed among the three groups. Future studies will include the investigation of long-term postoperative complications between low-energy and high-energy FLACS, and the correlation between the molecular findings and clinical outcomes including postoperative complications. Validation experiments for the identified proteins and metabolites will also be included in future studies.

In summary, our study demonstrated that FSL treatment in FLACS led to inflammatory and oxidative stress-related reactions, as well as subsequent dysfunction in mitochondrial fatty acid metabolism. These reactions were more apparent at a molecular level when the laser energy increased. These identified acylcarnitines, amino acids, and proteins hold promise as potential biomarkers for developing precautionary strategies and mitigating postoperative complications associated with FSL.

Acknowledgments

LZ thanks the support from InnoHK initiative and the Hong Kong Special Administrative Region Government.

Supported by Singapore National Medical Research Council (NMRC) Clinician Scientist Award (CSA) grant (MOH-CSAINV21jun-0001).

Disclosure: **C. Liu**, None; **X. Wang**, None; **H.S. Ong**, None; **M. Ang**, None; **S.-P. Chee**, None; **J. Ching**, None; **K.V. Chua**, None; **S.H.Y. Han**, None; **J.S. Mehta**, None; **L. Zhou**, None; **Y.-C. Liu**, None

References

1. Liu YC, Wilkins M, Kim T, Malyugin B, Mehta JS. Cataracts. *Lancet*. 2017;390(10094):600–612.
2. Abouzeid H, Ferrini W. Femtosecond-laser assisted cataract surgery: a review. *Acta Ophthalmol*. 2014;92(7):597–603.
3. Lim CW, Somani S, Chiu HH, Maini R, Tam ES. Astigmatic outcomes of single, non-paired intrastromal limbal relaxing incisions during femtosecond laser-assisted cataract surgery based on a custom nomogram. *Clin Ophthalmol*. 2020;14:1059–1070.
4. Kolb CM, Shajari M, Mathys L, et al. Comparison of femtosecond laser-assisted cataract surgery and conventional cataract surgery: a meta-analysis and systematic review. *J Cataract Refract Surg*. 2020;46(8):1075–1085.
5. Zhou KJ, Huang Y, Wang Y, et al. Safety and efficacy of cataract surgery performed with a low-energy femtosecond laser compared with conventional phacoemulsification in Chinese patients: a randomized clinical trial. *Eye Vis (Lond)*. 2023;10(1):31.
6. Sun H, Fritz A, Droge G, Neuhann T, Bille JF. Femtosecond-laser-assisted cataract surgery (FLACS). In: Bille JF (ed). *High resolution imaging in microscopy and ophthalmology: new frontiers in biomedical optics*. Cham, Switzerland; 2019:301–317.
7. Song X, Li L, Zhang X, Ma J. Comparing the efficacy and safety between femtosecond laser-assisted cataract surgery and conventional phacoemulsification cataract surgery: systematic review and meta-analysis. *Can J Ophthalmol*.

2024 20:S0008-4182(24)00172-8, doi: 10.1016/j.jcjo.2024.05.030. Online ahead of print.
8. Wang H, Chen X, Xu J, Yao K. Comparison of femtosecond laser-assisted cataract surgery and conventional phacoemulsification on corneal impact: a meta-analysis and systematic review. *PLoS One*. 2023;18(4):e0284181.
9. Xu J, Chen X, Wang H, Yao K. Safety of femtosecond laser-assisted cataract surgery versus conventional phacoemulsification for cataract: a meta-analysis and systematic review. *Adv Ophthalmol Pract Res*. 2022;2(1):100027.
10. Lin HY, Chuang YJ, Lin PJ. Surgical outcomes with high and low pulse energy femtosecond laser systems for cataract surgery. *Sci Rep*. 2021;11(1):9525.
11. Liu YC, Setiawan M, Ang M, Yam GHF, Mehta JS. Changes in aqueous oxidative stress, prostaglandins, and cytokines: comparisons of low-energy femtosecond laser-assisted cataract surgery versus conventional phacoemulsification. *J Cataract Refract Surg*. 2019;45(2):196–203.
12. Liu YC, Setiawan M, Chin JY, et al. Randomized controlled trial comparing 1-year outcomes of low-energy femtosecond laser-assisted cataract surgery versus conventional phacoemulsification. *Front Med (Lausanne)*. 2021;8(811093.
13. Stewart S, Liu YC, Setiawan M, et al. The effects of high energy capsulotomy on aqueous cytokine profiles and pupil size during femtosecond laser-assisted cataract surgery. *J Refract Surg*. 2022;38(9):587–594.
14. Toth G, Sandor GL, Kleiner D, et al. Evaluation of free radical quantity in the anterior chamber following femtosecond laser-assisted capsulotomy. *Orv Hetil*. 2016;157(47):1880–1883.
15. Masuda Y, Igarashi T, Oki K, Kobayashi M, Takahashi H, Nakano T. Free radical production by femtosecond laser lens irradiation in porcine eyes. *J Cataract Refract Surg*. 2019;45(8):1168–1171.
16. Al-Amrani S, Al-Jabri Z, Al-Zaabi A, Alshekaili J, Al-Khabori M. Proteomics: concepts and applications in human medicine. *World J Biol Chem*. 2021;12(5):57–69.
17. Luo Y, Cui HP, Liu Y, Chen L. Metabolomics and biomarkers in ocular matrix: beyond ocular diseases. *Int J Ophthalmol*. 2020;13(6):991–1003.
18. Teo AWJ, Zhang J, Zhou L, Liu YC. Metabolomics in corneal diseases: a narrative review from clinical aspects. *Metabolites*. 2023;13(3):380.
19. Li C, Wang Q, Ma J, et al. Integrative pathway analysis of genes and metabolites reveals metabolism abnormal subpathway regions and modules in esophageal squamous cell carcinoma. *Molecules*. 2017;22(10):1599.
20. Theodoridis K, Gika H, Kotali A. Acylcarnitines in ophthalmology: promising emerging biomarkers. *Int J Mol Sci*. 2022;23(24):16183.
21. Gali HE, Sella R, Afshari NA. Cataract grading systems: a review of past and present. *Curr Opin Ophthalmol*. 2019;30(1):13–18.
22. Mansoor H, Liu YC, Wong YR, Lwin NC, Seah XY, Mehta JS. Evaluation of femtosecond laser-assisted anterior capsulotomy in the presence of ophthalmic viscoelastic devices (OVDs). *Sci Rep*. 2020;10(1):21542.
23. Williams GP, Ang HP, George BL, et al. Comparison of intra-ocular pressure changes with liquid or flat applanation interfaces in a femtosecond laser platform. *Sci Rep*. 2015;5:14742.
24. Wu BM, Williams GP, Tan A, Mehta JS. A Comparison of different operating systems for femtosecond lasers in cataract surgery. *J Ophthalmol*. 2015;2015:616478.
25. Jabs DA, Nussenblatt RB, Rosenbaum JT; Standardization of Uveitis Nomenclature Working Group. Standardization of uveitis nomenclature for reporting clinical data. Results of the First International Workshop. *Am J Ophthalmol*. 2005;140(3):509–516.
26. Liu YC, Yam GHF, Lin MTY, et al. Comparison of tear proteomic and neuromediator profiles changes between small incision lenticule extraction (SMILE) and femtosecond laser-assisted in-situ keratomileusis (LASIK). *J Adv Res*. 2020;5(29):67–81.
27. Yam GH, Fuest M, Zhou L, et al. Differential epithelial and stromal protein profiles in cone and non-cone regions of keratoconus corneas. *Sci Rep*. 2019;9(1):2965.
28. Gao F, Kovalik JP, Zhao X, et al. Exacerbation of cardiovascular ageing by diabetes mellitus and its associations with acyl-carnitines. *Aging (Albany NY)*. 2021;13(11):14785–14805.
29. Tan NYT, et al. The glutamate-serine-glycine index as a biomarker to monitor the effects of bariatric surgery on non-alcoholic fatty liver disease. *Journal of the ASEAN Federation of Endocrine Societies*. 2024;39(2):54–60.
30. Ma W, Kim S, Chowdhury S, et al. DreamAI: algorithm for the imputation of proteomics data. *bioRxiv*. 2020;2020.2007.2021.214205.
31. Worley B, Halouska S, Powers R. Utilities for quantifying separation in PCA/PLS-DA scores plots. *Anal Biochem*. 2013;433(2):102–104.
32. Zhou Y, Zhou B, Pache L, et al. Metascape provides a biologist-oriented resource for the analysis of systems-level datasets. *Nat Commun*. 2019;10(1):1523.
33. Garcia-Moreno A, Lopez-Dominguez R, Villatoro-Garcia JA, et al. Functional enrichment analysis of regulatory elements. *Biomedicines*. 2022;10(3):590.
34. Safari-Alighiarloo N, Taghizadeh M, Rezaei-Tavirani M, Goliaei B, Peyvandi AA. Protein-protein interaction networks (PPI) and complex diseases. *Gastroenterol Hepatol Bed Bench*. 2014;7(1):17–31.
35. Pang Z, Zhou G, Ewald J, et al. Using MetaboAnalyst 5.0 for LC-HRMS spectra processing, multi-omics integration and covariate adjustment of global metabolomics data. *Nat Protoc*. 2022;17(8):1735–1761.
36. Singh A, Shannon CP, Gautier B, et al. DIABLO: an integrative approach for identifying key molecular drivers from multi-omics assays. *Bioinformatics*. 2019;35(17):3055–3062.
37. Rohart F, Gautier B, Singh A, Le Cao KA. mixOmics: an R package for 'omics feature selection and multiple data integration. *PLoS Comput Biol*. 2017;13(11):e1005752.
38. Yang Y, Yuan H, Yang T, et al. The expression regulatory network in the lung tissue of Tibetan Pigs provides insight into hypoxia-sensitive pathways in high-altitude hypoxia. *Front Genet*. 2021;12:691592.
39. Li B, Li S, Fan Y, et al. Computational analysis reveals the characteristics of immune cells in glomerular and tubulointerstitial compartments in IgA nephropathy patients. *Front Genet*. 2022;13:838863.
40. Pinazo-Duran MD, Shoaie-Nia K, Zanon-Moreno V, Sanz-Gonzalez SM, Del Castillo JB, Garcia-Medina JJ. Strategies to reduce oxidative stress in glaucoma patients. *Curr Neuropharmacol*. 2018;16(7):903–918.
41. Jridi I, Cante-Barrett K, Pike-Overzet K, Staal FJT. Inflammation and Wnt signaling: target for immunomodulatory therapy? *Front Cell Dev Biol*. 2020;8:615131.
42. Zhou B, Lin W, Long Y, et al. Notch signaling pathway: architecture, disease, and therapeutics. *Signal Transduct Target Ther*. 2022;7(1):95.
43. Hu Y, Pan Q, Zhou K, Ling Y, Wang H, Li Y. RUNX1 inhibits the antiviral immune response against influenza A virus through attenuating type I interferon signaling. *Virol J*. 2022;19(1):39.
44. Seth C, Mas C, Conod A, et al. Long-lasting WNT-TCF response blocking and epigenetic modifying activi-

ties of withanolide F in human cancer cells. *PLoS One*. 2016;11(12):e0168170.
45. Schwarzenbacher L, Schartmuller D, Leydolt C, Menapace R. Intraindividual comparison of cytokine and prostaglandin levels with and without low-energy, high-frequency femtosecond laser cataract pretreatment after single-dose topical NSAID application. *J Cataract Refract Surg*. 2020;46(8):1086–1091.
46. Riau AK, Liu YC, Lwin NC, et al. Comparative study of nJ- and muJ-energy level femtosecond lasers: evaluation of flap adhesion strength, stromal bed quality, and tissue responses. *Invest Ophthalmol Vis Sci*. 2014;55(5):3186–3194.
47. Mirshahi A, Ponto KA. Changes in pupil area during low-energy femtosecond laser-assisted cataract surgery. *J Ophthalmic Vis Res*. 2019;14(3):251–256.
48. Van Nuffel S, Claeys MF, Claeys MH. Cystoid macular edema following cataract surgery with low-energy femtosecond laser versus conventional phacoemulsification. *Clin Ophthalmol*. 2020;14:2873–2878.
49. Berk TA, Schlenker MB, Campos-Moller X, Pereira AM, Ahmed IIK. Visual and refractive outcomes in manual versus femtosecond laser-assisted cataract surgery: a single-center retrospective cohort analysis of 1838 eyes. *Ophthalmology*. 2018;125(8):1172–1180.
50. Yoshida Y, Yamagishi S, Ueda S, Yoshimura K, Okuda S, Yamakawa R. Aqueous humour levels of asymmetric dimethylarginine (ADMA) are correlated with pigment epithelium-derived factor (PEDF) in patients with uveitis. *J Int Med Res*. 2007;35(6):892–895.
51. Wei P, He M, Teng H, Han G. Metabolomic analysis of the aqueous humor from patients with central retinal vein occlusion using UHPLC-MS/MS. *J Pharm Biomed Anal*. 2020;188:113448.
52. Suwannasom N, Kao I, Pruss A, Georgieva R, Baumler H. Riboflavin: the health benefits of a forgotten natural vitamin. *Int J Mol Sci*. 2020;21(3):950.
53. Ronchi JA, Francisco A, Passos LA, Figueira TR, Castilho RF. The contribution of nicotinamide nucleotide transhydrogenase to peroxide detoxification is dependent on the respiratory state and counterbalanced by other sources of NADPH in Liver mitochondria. *J Biol Chem*. 2016;291(38):20173–20187.
54. Derakhshani A, Safarpour H, Abdoli Shadbad M, et al. The role of hemoglobin subunit delta in the immunopathy of multiple sclerosis: mitochondria matters. *Front Immunol*. 2021;12:709173.
55. Stempel D, Sandusky H, Lampi K, et al. BetaB1-crystallin: identification of a candidate ciliary body uveitis antigen. *Invest Ophthalmol Vis Sci*. 2003;44(1):203–209.
56. Balasubramanian P, Vijayarangam V, Deviparasakthi MKG, et al. Implications and progression of peroxiredoxin 2 (PRDX2) in various human diseases. *Pathol Res Pract*. 2024;254:155080.
57. Chhunchha B, Singh P, Stamer WD, Singh DP. Prdx6 retards senescence and restores trabecular meshwork cell health by regulating reactive oxygen species. *Cell Death Discov*. 2017;3:17060.
58. Wickstrom K, Lundgren B, Torngren L, Ostberg C. Aqueous humor polyamines and alkaline phosphatase activity in endotoxin-induced uveitis: correlations to diverse leukocyte subsets. *Ophthalmic Res*. 1992;24(3):175–180.
59. Mhatre S, Opere CA, Singh S. Unmet needs in glaucoma therapy: the potential role of hydrogen sulfide and its delivery strategies. *J Control Release*. 2022;347:256–269.
60. von Arnim CA, Timmler M, Ludolph AC, Riepe MW. Adenosine receptor up-regulation: initiated upon preconditioning but not upheld. *Neuroreport*. 2000;11(6):1223–1226.
61. Ramkumar V, Hallam DM, Nie Z. Adenosine, oxidative stress and cytoprotection. *Jpn J Pharmacol*. 2001;86(3):265–274.
62. Gowtham L, Halder N, Angmo D, et al. Elevated histamine levels in aqueous humor of patients with glaucoma. *Mol Vis*. 2021;27:564–573.
63. Hu RG, Zhu Y, Donaldson P, Kalloniatis M. Alterations of glutamate, glutamine, and related amino acids in the anterior eye secondary to ischaemia and reperfusion. *Curr Eye Res*. 2012;37(7):633–643.
64. Strand E, Pedersen ER, Svingen GF, et al. Serum acylcarnitines and risk of cardiovascular death and acute myocardial infarction in patients with stable angina pectoris. *J Am Heart Assoc*. 2017;6(2):e003620.
65. Koh AS, Gao F, Tan RS, et al. Metabolomic correlates of aerobic capacity among elderly adults. *Clin Cardiol*. 2018;41(10):1300–1307.
66. Zhu Y, He H. Molecular response of mitochondria to a short-duration femtosecond-laser stimulation. *Biomed Opt Express*. 2017;8(11):4965–4973.
67. Han G, Wei P, He M, Teng H, Chu Y. Metabolomic profiling of the aqueous humor in patients with wet age-related macular degeneration using UHPLC-MS/MS. *J Proteome Res*. 2020;19(6):2358–2366.
68. Paris LP, Johnson CH, Aguilar E, et al. Global metabolomics reveals metabolic dysregulation in ischemic retinopathy. *Metabolomics*. 2016;12:15.
69. Mitchell SL, Ma C, Scott WK, et al. Plasma metabolomics of intermediate and neovascular age-related macular degeneration patients. *Cells*. 2021;10(11):3141.
70. Moon SJ, Dong W, Stephanopoulos GN, Sikes HD. Oxidative pentose phosphate pathway and glucose anaplerosis support maintenance of mitochondrial NADPH pool under mitochondrial oxidative stress. *Bioeng Transl Med*. 2020;5(3):e10184.
71. Xiong Y, Lei QY, Zhao S, Guan KL. Regulation of glycolysis and gluconeogenesis by acetylation of PKM and PEPCK. *Cold Spring Harb Symp Quant Biol*. 2011;76:285–289.

Investigative Ophthalmology & Visual Science